ChemComm

COMMUNICATION

View Article Online
View Journal | View Issue



Cite this: *Chem. Commun.*, 2019, 55, 12809

Received 7th August 2019,
Accepted 27th September 2019

DOI: 10.1039/c9cc06123a

rsc.li/chemcomm



# Reversible transformation between $CsPbBr_3$ nanowires and nanoparticles†

Yongqiang Ji, [a] Minqiang Wang,*[a] Zhi Yang, [a] Shangdong Ji,[a] Hengwei Qiu, [a] Jinjuan Dou[a] and Nikolai V. Gaponenko[b]

**We show that $CsPbBr_3$ nanowires (NWs) are formed by the hierarchical arrangement of individual nanoparticles (NPs), and reversible transformation from NWs to NPs is also achieved by anion exchange.**

Among the leading energy materials, metal halide perovskite (MHP) nanocrystals (NCs) remain at the forefront of current research. The exciting feature of these NCs is their unprecedented high photoluminescence quantum yields (PLQYs) and narrow emission band, which is extensively studied and optimized during their synthesis as well as post-synthesis modifications.[1] Compared with traditional metal-chalcogenide NCs, MHP NCs possess unique characteristics of wide colour tenability *via* post-synthesis anion exchange with good photochemical stability even without shell coating.[2] These properties make MHPs promising materials not only for light-emitting diode applications but also for other optoelectronic devices with enhanced performance,[3] such as solar cells,[4] photoconductor detectors,[5] and lasers.[6] Despite tremendous progress in photoelectric devices, many challenges, including growth mechanism and rational morphology control, should be settled before they can be applied in practical fields.

Very recently, high aspect ratio NWs have attracted significant attention due to their potential applications in many optoelectronic devices.[7,8] For example, NWs can provide dominant carrier transport pathways, which is an ideal electronic property for fabricating high-efficiency solar cells. Therefore, the understanding of the formation mechanism of MHP NWs is crucially important for further optimizing their synthesis. On the one hand,[9–13] Sardar's group found that formation of MHP NWs was attributed to the assembly of spherical NCs.[10] However, the formation of NWs with good PLQYs takes too long. Wan *et al.* reported the synthesis of $CsPbI_3$ NPs and demonstrated how these NCs self-assemble into NWs immediately.[11] While saving time in operation was shown with this approach, the self-assembly process leads to phase transitions, thus losing the expected properties. Liu's groups developed a light-induced assistance method that allows $CsPbBr_3$ NCs to self-assemble into NWs while preserving their cubic phase.[12] However, such methods are believed to suffer from the requirement of significant laboratory infrastructures. On the other hand, Lee *et al.* showed that silver NWs can convert into NPs.[13] Besides, it was also found that the reversible transformation between different phase MHP NCs can be achieved by special treatment.[14,15] However, all the reported transformation pathways between NPs and NWs just occur in one fixed direction. To the best of our knowledge, a reversible method in morphology from NPs to NWs and then back to NPs has not been investigated thus far.

In this communication, we report the synthesis of monodisperse $CsPbBr_3$ NPs with ~3.0 nm diameters, which are assembled into NWs by the hierarchical arrangement of individual NPs. Furthermore, a reversible transformation from NWs to NPs can be achieved *via* anion exchange.

A reversible transformation from NPs to NWs and then back to NPs is clearly shown in Fig. 1. To illustrate the detailed process of reversible transformation, synthetic NCs were firstly characterized by Transmission electron microscopy (TEM). The product typically consists of uniform and ultrathin NWs. As indicated by TEM, the thickness of the NWs is estimated to be

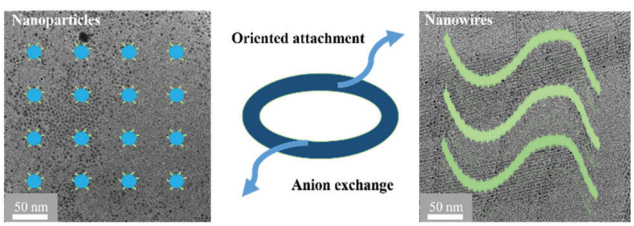


Fig. 1 Schematic diagram of reversible transformation between NWs and NPs.

[a] *Electronic Materials Research Laboratory (EMRL), Key Laboratory of Education Ministry, International Center for Dielectric Research (ICDR), Shanxi Engineering Research Center of Advanced Energy Materials and Devices, School of Electronic and Information Engineering, Xi'an Jiaotong University, Xi'an 710049, China. E-mail: mqwang@xjtu.edu.cn*

[b] *Belarusian State University of Informatics and Radioelectronics, P. Browki St. 6, 220013 Minsk, Belarus*

† Electronic supplementary information (ESI) available. See DOI: 10.1039/c9cc06123a

only a few unit-cell-thick, and its length is about over a hundred nanometers (ESI,† Fig. S1a). Because the thickness of NWs is smaller than their Bohr radius (7 nm),[16,17] a strong fluorescence can be observed in the inset of the ESI,† Fig. S1e. Furthermore, the optical absorption and steady-state PL spectra of the synthesized $CsPbBr_3$ NWs display peaks at 437 nm and 454 nm, respectively (ESI,† Fig. S1e). The X-ray diffraction (XRD) pattern shows that most of the peaks conform to cubic phase standard card (PDF #54-0752) well. Although some of the interference peaks correspond to the hexagonal phase standard card (PDF #73-2468), it still indicates that the product is a cubic phase (ESI,† Fig. S1f).[18] As the concentration of NWs increases, these NWs tend to be self-assembled into bundles on TEM grids (ESI,† Fig. S1b–d). Upon careful inspection of the magnified TEM images of the NWs (ESI,† Fig. S2), it is apparent that many spherical NPs with a much darker contrast, are decorating their body. Some people think that the bright particles are Pb particles generated through *in situ* reduction of $CsPbBr_3$ NWs.[19,20] While others believe that the bright particles are MHP NPs, which are assembled into NWs.[9,10]

Since spherical NPs were found on the NW surface, the reaction time was reduced to trace back to its source by time-dependent TEM. The 5 s reaction sample displays nearly monodispersed, ultrasmall spherical $CsPbBr_3$ NPs with $3.2 \pm 0.2$ nm diameter (Fig. 2a and g). These results strongly support self-assembly and an oriented attachment growth process where, at the early stages of synthesis, ultrasmall NPs formed first. After another 5 s, two or more NPs are fused to form tadpole-like nanorods (t-NRs) with one or two enlarged spherical ends. The width of the t-NRs is measured to be around $\sim$3 nm, while their length varies from $\sim$2 to 10 nm (Fig. 2b). Therefore, we believe that t-NRs are formed by the ''oriented attachment'' of spherical NPs. Similar behaviour was previously observed in silver NWs.[21] With the time of 30 s, the spherical ends of t-NRs became smaller or even disappeared, and all NCs become NRs (Fig. 2c and h). Magnified images are shown in the ESI,† Fig. S3, where these NRs were observed to be around 20–30 nm in length and $\sim$3 nm in width. With the extension of time, these NRs disappeared, and some NWs with a diameter of 3 nm and large aspect ratios (with length varying from $\sim$100 to 500 nm) are formed (Fig. 2d and e). In addition, some comb-like nanostructures also are found, which may originate from some NRs sharing the same crystallographic orientation in the junction regions with a large angle mismatch (ESI,† Fig. S4).[22] After the solution is aged for 5 min, all NCs become NWs with a length up to hundreds of nanometers (Fig. 2f and i). It is obvious that the length of the NWs increases significantly with no apparent increase in their diameter, and there is a significant reduction in the number of small particles that are seen (Fig. 2a–f). Furthermore, several shaped NCs corresponding to the formation of NWs are found on carbon-coated TEM copper by high-resolution TEM (HRTEM). The NRs with one or two enlarged spherical ends (ESI,† Fig. S5a) may consist of NPs (ESI,† Fig. S5b), and then directionally connect each other and eventually lead to the formation of NWs (ESI,† Fig. S5c), as the morphology depicts in the ESI,† Fig. S5. As the reaction time increases further, the thickness of the NWs becomes thicker and results in redshift of the PL maximum up to dozens of nanometers (ESI,† Fig. S6 and S7). Based on the above observation, a possible mechanism of plausible nucleation and growth of $CsPbBr_3$ NWs in terms of the thermodynamics is proposed and schematically described in the ESI,† Fig. S8. Initially, these $CsPbBr_3$ nanoclusters grow from dissolved metal–ligand complexes to sphere $CsPbBr_3$ NPs. According to the Gibbs–Thomson equation, these NPs become unstable and tend to aggregate as they grow to a critical size.[9] To reduce the overall energy, these NPs begin to attach through the facets with the highest surface energy and form NWs. As time further increased, these NWs approach each other to expand their width.

With the morphological evolution from NPs to NWs, the absorption peak shifts to a higher wavelength, and the colour of the solution gradually changes from blue to green under UV light (ESI,† Fig. S9b). One can see the emergence of the absorption peak corresponding to NPs at 398 nm (Fig. 3a). With increasing

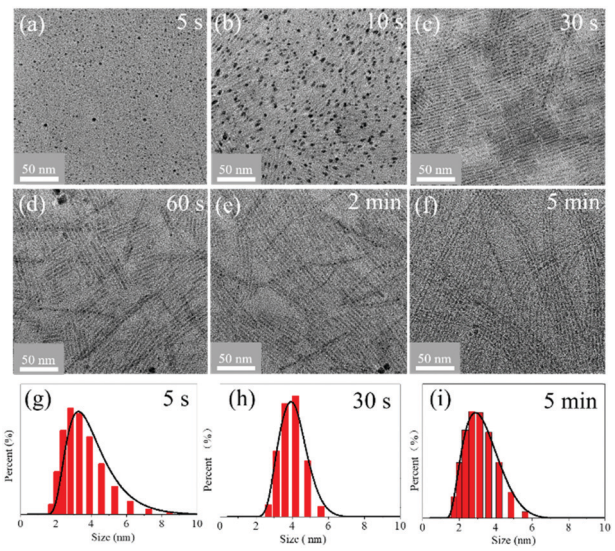


Fig. 2 TEM images showing the time evolution of the morphology with aging time: (a) 5 s. (b) 10 s. (c) 30 s. (d) 60 s. (e) 2 min. (f) 5 min. Histogram of size analysis of NWs: (g) 5 s. (h) 30 s. (i) 5 min.

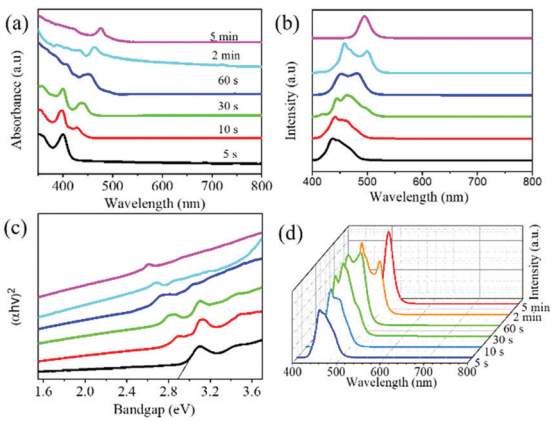


Fig. 3 (a) Absorption, (b) PL, (c) bandgap and (d) PL intensity of $CsPbBr_3$ NWs with different reaction times.

aging time, the intensity of the absorption peaks corresponding to NWs at 427 nm progressively increases and redshifts, while the peak at 398 nm diminishes and disappears. The change in the peak position is further confirmed by the increase in lifetime and bandgap (ESI,† Fig. S9a, c and Fig. 3c). Accompanying the morphology transformation, the PLQY initially increases from 42% to 60%, then decreases to 54% (ESI,† Fig. S9d). Correspondingly, the intensity of the PL peak at higher energy decreases, and those of the peaks at higher wavelength appear and become stronger (Fig. 3b and d). This PL switch confirms the conversion of NPs to NWs. The conversion of $CsPbBr_3$ NPs to NWs completes within 5 min as indicated by the vanished peaks at high energy direction.

Although extending the growth time can lead to the morphology changing from NPs to NWs, it requires lots of time, energy input, and laborious effort and thus increases the costs of production. It was reported that polar solvent can rapidly induce self-assembly of $CsPbI_3$ NPs into NWs.[11] To determine whether or not added polar solvent can lead to a rapid broadening of NWs, some ethanol is introduced into the NW solution. The colour of the solution changing from yellow-green to green could be immediately observed under UV light (ESI,† inset Fig. S10). After the introduction of ethanol, the structure deformation and crystal polarization cause the decrease of surface energy and the detachment of surface ligands, leading to the decline of steric repulsion among the NWs. Meanwhile, the dipole–dipole attraction and orientation force will attract them closer. The spacing of adjacent NWs gradually shrinks over time. Once adjacent NWs get attached, they fuse to form a wider NW (ESI,† Fig. S10), like what occurs in the oriented attachment of NPs.[9] As depicted in Fig. 4, two or more thin NWs are fused to form a thick NW through an oriented attachment process (Fig. 4a–c). These thick NWs attract each other and combine into thicker ones (Fig. 4c and d), and further merge with other NWs, leading to even thicker ones (Fig. 4e and f). Furthermore, the preformed NW parts have a chance to attach and merge with others

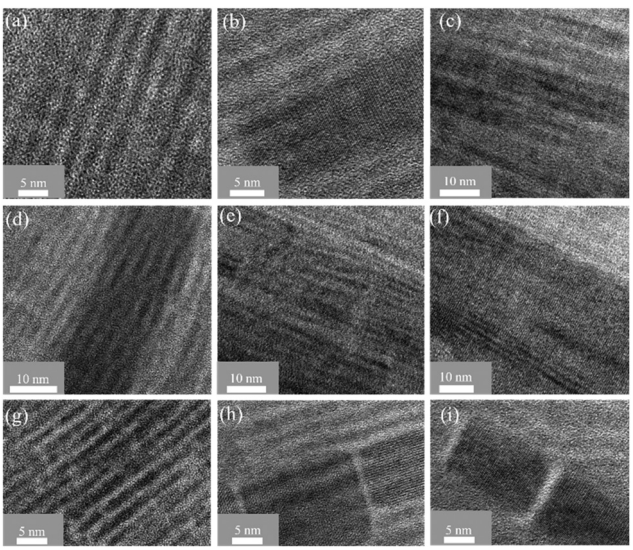


Fig. 4 As self-assembly progresses, the morphology of the $CsPbBr_3$ NWs changes. (a–f) Variations from thin l-NWs to thick l-NWs. (g–i) Changes from s-NWs to nanosheets.

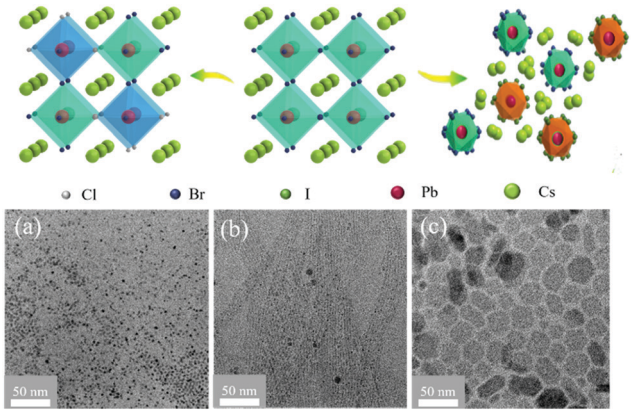


Fig. 5 Schematic diagram of anion exchange (top). (a) TEM image of $Cl^-$ exchange NWs. (b) TEM image of initial NWs. (c) TEM image of $I^-$ exchange NWs.

while each NW can still attract NWs and keep growing. Through the self-assembly and fusion process, the final NW width can reach up to dozens of nanometers. Moreover, strong polar solvents usually accelerate the self-assembly process and rapidly form thicker NWs. Interestingly, NWs with different thickness are found to have the same lattice space of 0.42 nm corresponding to the 110 lattice spacing. This indicates that the preferred oriented attachment growth axis of the NWs is along the [110] direction of the cubic structure (ESI,† Fig. S11). More importantly, it is found that the well-known cubic shaped perovskite nanosheets may be attributed to s-NW self-assembly, which is evidenced by TEM images (Fig. 4g–i and ESI,† Fig. S12).

Interestingly, for the NWs the formation process is fully reversible, and by an anion-exchange process again to the original conditions, NPs with different morphologies can be regained (Fig. 5), which is similar to the reverse process of oriented attachment. These NWs become sphere NPs with a $\sim$5 nm size by treatment with TBA-Cl (Fig. 5a) and show a clear lattice spacing of 0.42 nm, which can be indexed as the (110) plane of cubic $CsPbBr_3$ (ESI,† Fig. S13a). While NWs become hexagon-shaped NPs with a $\sim$20 nm size, also known as 0D MHP NCs,[23] through treatment with TBA-I (Fig. 5d and ESI,† Fig. S13b). This indicates that in a network of NWs there exist some inter-wire junctions, and these junction regions are disconnected by anion-exchange, thereby producing NPs, which are the same as the NPs obtained directly using the precursor. Additionally, the optical properties of the $CsPbBr_3$ NWs before and after the anion exchange were characterized (ESI,† Fig. S14). The fluorescence peak at 457 nm for $CsPbBr_3$ NWs is redshifted with increasing iodide content and blue-shifted as the chloride content is increased. However, regardless of how the source of iodine is added, the fluorescence peak is always around 580 nm. This may be because 0D perovskite has a more stable $(PbBr_6)^{4-}$ structure than that of 3D perovskite, thus suppressing anion exchange.

In summary, we realize a reversible transformation between NPs and NWs through simple treatments. This transformation is the first report of direct reversibility between $CsPbBr_3$ NPs and NWs where the cubic morphology of the $CsPbBr_3$ NCs

before and after the whole cycle is preserved or altered by different halogens.

We thank Ms Yu Wang at Instrument Analysis Center of Xi'an Jiaotong University for her help with PL analysis. This work was supported by the National Natural Science Foundation of China (NSFC, 61774124, 51572216 and 61604122), the Fundamental Research Funds for the Central Universities (1191329876 and 1191329152), the 111 Plan (B14040) and the China Postdoctoral Science Foundation (2017M613139).

## Conflicts of interest

There are no conflicts to declare.

## References

1 Y. Zhang, J. Liu, Z. Wang, Y. Xue, Q. Ou, L. Polavarapu, J. Zheng, X. Qi and Q. Bao, *Chem. Commun.*, 2016, **52**, 13637–13655.
2 J. Cai, K. Gu, Y. Zhu, J. Zhu, Y. Wang, J. Shen, A. Trinchi, C. Li and G. Wei, *Chem. Commun.*, 2018, **54**, 8064–8067.
3 H. Hu, L. Wu, Y. Tan, Q. Zhong, M. Chen, Y. Qiu, D. Yang, B. Sun, Q. Zhang and Y. Yin, *J. Am. Chem. Soc.*, 2018, **140**, 406–412.
4 E. M. Sanehira, A. R. Marshall, J. A. Christians, S. P. Harvey, P. N. Ciesielski, L. M. Wheeler, P. Schulz, L. Y. Lin, M. C. Beard and J. M. Luther, *Sci. Adv.*, 2017, **3**, eaao4204.
5 Z. Yang, J. Dou, M. Wang, J. Li, J. Huang and J. Shao, *J. Mater. Chem. C*, 2018, **6**, 6739–6746.
6 L. Zhang, F. Yuan, H. Dong, B. Jiao, W. Zhang, X. Hou, S. Wang, Q. Gong and Z. Wu, *ACS Appl. Mater. Interfaces*, 2018, **10**, 40661–40671.
7 M. Shoaib, X. Zhang, X. Wang, H. Zhou, T. Xu, X. Wang, X. Hu, H. Liu, X. Fan, W. Zheng, T. Yang, S. Yang, Q. Zhang, X. Zhu, L. Sun and A. Pan, *J. Am. Chem. Soc.*, 2017, **139**, 15592–15595.
8 D. Yang, Y. Zou, P. Li, Q. Liu, L. Wu, H. Hu, Y. Xu, B. Sun, Q. Zhang and S. Lee, *Nano Energy*, 2018, **47**, 235–242.
9 Y. Liu, M. Guo, S. Dong, X. Jiao, T. Wang and D. Chen, *J. Mater. Chem. C*, 2018, **6**, 7797–7802.
10 M. B. Teunis, A. Jana, P. Dutta, M. A. Johnson, M. Mandal, B. B. Muhoberac and R. Sardar, *Chem. Mater.*, 2016, **28**, 5043–5054.
11 J. K. Sun, S. Huang, X. Z. Liu, Q. Xu, Q. H. Zhang, W. J. Jiang, D. J. Xue, J. C. Xu, Y. J. Ma, J. Ding, Q. Q. Ge, L. Gu, X. H. Fang, H. Z. Zhong, J. S. Hu and L. J. Wan, *J. Am. Chem. Soc.*, 2018, **140**, 11705–11715.
12 J. Liu, K. Son, Y. Shi, X. Liu, J. Chen, K. X. Yao, J. Pan, C. Yang, J. Yin, L. Xu, H. Yang, A. M. El-Zohry, B. Xin, S. Mitra, M. N. Hedhili, I. S. Roqan, O. F. Mohammed, Y. Han and O. M. Bakr, *Chem. Mater.*, 2019, **31**, 6642–6649.
13 H. Oh, J. Lee and M. Lee, *Appl. Surf. Sci.*, 2018, **427**, 65–73.
14 W. Shen, L. Ruan, Z. Shen and Z. Deng, *Chem. Commun.*, 2018, **54**, 2804.
15 Y. Li, H. Huang, Y. Xiong, S. V. Kershaw and A. L. Rogach, *CrystEngComm*, 2018, **20**, 4900–4904.
16 S. G. Carrero, L. Baren, E. Debroye, C. Martin, P. Bondia, C. Flors, R. E. Galian, J. Hofkens and J. P. Prieto, *Chem. Commun.*, 2019, **55**, 2968–2971.
17 D. Zhang, Y. Yu, Y. Bekenstein, A. B. Wong, A. P. Alivisatos and P. Yang, *J. Am. Chem. Soc.*, 2016, **138**, 13155–13158.
18 Y. ji, M. Wang, Z. Yang, S. Ji and H. Qiu, *J. Mater. Chem. C*, 2019, **7**, 8471–8476.
19 H. Huang, M. Liu, J. Li, L. Luo, J. Zhao, Z. Luo, X. Wang, Z. Ye, H. He and J. Zeng, *Nanoscale*, 2017, **9**, 104–108.
20 A. Kostopoulou, M. Sygletou, K. Brintakis, A. Lappas and E. Stratakis, *Nanoscale*, 2017, **9**, 18202–18207.
21 H. Feng, Y. Yang, Y. You, G. Li, J. Guo, T. Yu, Z. Shen, T. Wub and B. Xing, *Chem. Commun.*, 2009, 1984–1986.
22 J. Fang, S. Du, S. Lebedkin, Z. Li, R. Kruk, M. Kappes and H. Hahn, *Nano Lett.*, 2010, **10**, 5006–5013.
23 C. Jia, H. Li, X. Meng and H. Li, *Chem. Commun.*, 2018, **54**, 6300–6303.

 